PROCEEDINGS OF SCIENCE

High-precision nuclear forces: Where do we stand?

Evgeny Epelbaum[*†]
Ruhr-Universität Bochum, Fakultät für Physik und Astronomie, Institut für Theoretische Physik II, D-44780 Bochum, Germany
E-mail: evgeny.epelbaum@rub.de

Chiral effective field theory is being developed into a precision tool for low-energy nuclear physics. I review the state of the art in the two-nucleon sector, discuss applications to few-nucleon systems and outline future directions in this field.

The 9th International workshop on Chiral Dynamics
17-21 September 2018
Durham, NC, USA

[*] Speaker.

[†] It is a great pleasure to thank my collaborators Hermann Krebs, Ulf-G. Meißner, Patrick Reinert and all members of the LENPIC collaboration for sharing their insights into the discussed topics. I am also grateful to Daniel Phillips for useful discussions of the Bayesian approach. Finally, I thank the organizers of CD2018 for making this exciting workshop possible. This work was supported in part by DFG (SFB/TR 110, “Symmetries and the Emergence of Structure in QCD”) and the BMBF (Grant No. 05P18PCFP1).

PoS(CD2018)006

1. Introduction

Chiral effective field theory (EFT) is currently the most efficient approach to nuclear forces and current operators which is widely used to study low-energy nuclear structure and reactions. There have been a remarkable progress towards developing this method into a precision tool. By pushing the chiral expansion of the nuclear Hamiltonian to fifth order (N^4LO) and even beyond, it, for the first time, became possible to perform a high-precision partial wave analysis (PWA) of neutron-proton (np) and proton-proton (pp) scattering data below the pion production threshold [1] in the framework of chiral EFT. In parallel with these developments, a simple universal algorithm for estimating truncation uncertainties was formulated in Ref. [2] and applied to a broad range of reactions/observables [3, 4, 5, 6, 7, 8, 9, 10]. In Refs. [11, 12, 13], this algorithm was statistically validated and further developed using the Bayesian approach. These developments, coupled with ab initio few- and many-body methods, provide a solid basis for establishing a reliable and predictive approach to low-energy nuclear physics in the framework of chiral EFT.

In this contribution I review the current status of the NN sector, discuss selected applications of chiral EFT to heavier systems and outline some challenges to be addressed in the coming years. This paper is organized as follows. In section 2 I review our recent work on high-precision NN chiral potentials and the PWA of NN scattering data. Selected applications beyond the NN system are discussed in section 3, while section 4 is devoted to the Bayesian approach for estimating truncation errors. Finally, section 5 provides a brief summary and gives the outlook on ongoing and future research in this field.

2. High-precision NN chiral forces at N^4LO^+

The most recent chiral NN potentials developed by our group [1, 2, 3] feature a number of important differences as compared to the next-to-next-to-next-to-leading order (N^3LO) interactions of Ref. [14], which are summarized below.

- The chiral expansion has been pushed to N^4LO. Furthermore, to describe certain very precisely measured proton-proton polarization observables it was necessary to include four sixth-order (N^5LO) contact interactions contributing to F-waves, as it was also done in Ref. [15]. The resulting NN potentials are referred to as N^4LO^+.

- The long-range part of the nuclear force stemming from pion-exchange is regularized with a *local* regulator either in coordinate [2, 3] or in momentum space [1]. The usage of local regulators allows one reduce finite-cutoff artifacts by maintaining the model-independent long-range part of the interaction which governs the near-threshold energy behavior of the scattering amplitude. In particular, when expanded in (inverse) powers of the coordinate- (momentum-) space cutoff R (Λ), the regulators employed in Refs. [1, 2, 3] do not induce any long-range artifacts. At the same time, contrary to the nonlocal regulators used e.g. in [14, 15, 16], the local ones cut off precisely the unwanted short-range components of the pion exchange contributions which cannot be described reliably in chiral EFT. The momentum-space version of the local regulator in [1] is particularly well suited for applications to many-body forces and exchange currents [17]. For a discussion of regulator artifacts in uniform nuclear matter see Ref. [18].

PoS(CD2018)006

- All low-energy constants (LECs) entering the long-range part of the interaction have been taken from matching the chiral expansion of the pion-nucleon scattering amplitude at the subthreshold point to the solution of the Roy-Steiner equations [19]. The resulting long-range nuclear forces and exchange currents are thus fixed in a parameter-free way by the spontaneously broken chiral symmetry of QCD and experimental information on the pion-nucleon and pion-pion systems.

- Contrary to the potentials of Ref. [2, 3, 14], the LECs accompanying the NN short-range interactions were extracted from np and pp scattering data rather than from the Nijmegen PWA. Specifically, we employed the self-consistent 2013 Granada database [20] which includes 2996 pp and 3717 np mutually consistent scattering data (including normalizations) below $E_{\rm lab} = 350$ MeV.

- We found that three out of fifteen NN contact interactions at N^{3}LO used e.g. in [2, 3, 14, 15, 16] are redundant and can be eliminated by performing suitable unitary transformations. Eliminating such redundant operators was, in fact, essential to perform converged fits to NN scattering data. Choosing specific strength of the redundant contact interactions fixes the off-shell behavior of the NN potential at this chiral order. Different choices lead to the same observables (modulo corrections starting from N^{5}LO) but may strongly affect the perturbativeness of the interactions and other features such as e.g. the expectation value of the kinetic energy in the deuteron, which are not observable. The choice of the redundant contact interactions employed in [1] leads to soft NN potentials in contrast with the interactions of Ref. [2, 3], which acquire strong repulsive contributions at N^{3}LO that manifest themselves in a significant underbinding of light nuclei if calculated without inclusion of the corresponding three-body forces [4, 6]. With the "soft" choice for the redundant contact interactions in [1], all LECs accompanying the short-range operators are found to be of natural size for all considered values of the ultraviolet (UV) cutoff. In contrast, some of the LECs contributing to the ^{1}S$_0$ and ^{3}S$_1$-^{3}D$_1$ channels at N^{3}LO and beyond were found to take rather large values in Refs. [2, 3, 14, 16]. I expect this also to be the case for the recent potentials of Ref. [15].

- Finally, a careful uncertainty analysis was carried out in Ref. [1]. In addition to the truncation error, see the discussion in section 4, this paper provides the analysis of statistical uncertainties and the errors associated with pion-nucleon LECs and the choice of the energy range when fitting NN scattering data. The covariance matrix available for the potentials of Ref. [1] allows one to propagate statistical uncertainties in a straightforward way when calculating arbitrary observables, see Ref. [21] for a related discussion.

The resulting chiral NN potentials at N^{4}LO$^+$ of Ref. [1] provide excellent description of NN scattering data below pion production threshold, which is comparable to or even better then that obtained from high-precision phenomenological potentials such as CD Bonn [22], Nijm I,II and Reid 93 [23]. For the first time, the potentials derived in chiral EFT qualify to be regarded as PWA. The important role of the two-pion exchange, which is completely determined by the spontaneously broken approximate chiral symmetry of QCD along with the experimental information on the pion-nucleon system, manifests itself in the reduction of the number of adjustable parameters by $\sim 40\%$

Table 1: χ^2/datum for the description of the np and pp scattering data for the potentials of Ref. [1] based on the cutoff value of $\Lambda = 450$ MeV at all considered chiral orders.

	LO	NLO	N^{2}LO	N^{3}LO	N^{4}LO	N^{4}LO$^+$
$\chi^2/\text{datum}\,(np,\ 0-300\ \text{MeV})$	75	14	4.1	2.01	1.16	1.06
$\chi^2/\text{datum}\,(pp,\ 0-300\ \text{MeV})$	1380	91	41	3.43	1.67	1.00

as compared with the phenomenological potentials. Further evidence of the chiral two-pion exchange is provided by a significant reduction of the χ^2 per datum for the description of np and pp data when gong from NLO to N^{2}LO and from N^{3}LO to N^{4}LO as shown in Table 1, which is achieved solely due to the inclusion of the corresponding parameter-free long-range terms.[1]

The chiral NN potentials of Ref. [1] are available for five different choices of the UV cutoff, namely $\Lambda = 350$, 400, 450, 500 and 550 MeV. The appearance of a *finite* cutoff that needs to be kept of the order of the breakdown scale [24, 25, 26, 27, 28] is an unavoidable feature of the employed non-relativistic approach with the scattering amplitude being generated non-perturbatively by solving the Schrödinger or Lippmann-Schwinger equations for a potential truncated at a finite chiral order, see Ref. [29] for a discussion of some common misconceptions in connection with non-perturbative renormalization of chiral EFT for the two-nucleon system. To the best of my knowledge, the only available approach which allows one to eliminate the UV cutoff in calculations based on the non-perturbative treatment of the one-pion exchange potential in the way compatible with the principles of EFT is the one proposed in Ref. [30], see Refs. [31, 32, 33, 34, 34, 35] for selected applications. With the exception of Ref. [36], this framework, however, has not yet been applied beyond leading order.

Clearly, the adopted finite-cutoff formulation of chiral EFT leads unavoidably to residual cutoff-dependence in calculated observables, which reflects the impact of contact interactions beyond the truncation order. In Fig. 1, the dependence of the χ^2 per datum is shown at N^{4}LO$^+$ as function of the cutoff value. One The significant increase in χ^2 per datum for the softest considered cutoff value of $\Lambda = 350$ MeV reflects the fact that this soft cutoff gets close to the center-of-mass momentum $p = 307$ MeV corresponding to $E_{\rm lab} = 200$ MeV. For larger considered cutoff values, the residual Λ-dependence appears to be rather small for the N^{4}LO$^+$ potentials of Ref. [1]. The significantly larger values of χ^2 per datum and the stronger Λ-dependence for the potentials of Ref. [15] at the same chiral order are consistent with larger cutoff artifacts induced by the nonlocal regulator used in that paper.

Finally, it is reassuring to note a rather good convergence of the chiral expansion in the NN sector. As a characteristic example, the chiral expansion of the total np cross section at $E_{\rm lab} =$ 150 MeV for the medium cutoff $\Lambda = 450$ MeV takes the form

$$\sigma_{\rm tot} \,=\, 51.4_{\rm LO} \,-\, 3.0_{\rm NLO} \,+\, 1.7_{\rm N^2LO} \,+\, 0.5_{\rm N^3LO} \,+\, 0.4_{\rm N^4LO} \,+\, 0.1_{\rm N^4LO^+}\,, \tag{2.1}$$

leading to the final result of $\sigma_{\rm tot}^{\rm N^4LO^+} = 51.10(12)(39)(19)(6)$ mb to be compared with the experimental data of $\sigma_{\rm tot}^{\rm exp} = 51.02(30)$ mb [37]. The quoted errors for the theoretical result are our

[1] At N^{4}LO, the observed improvement also reflects the inclusion of an additional isospin-breaking contact interaction in the ^{1}S$_0$ channel.

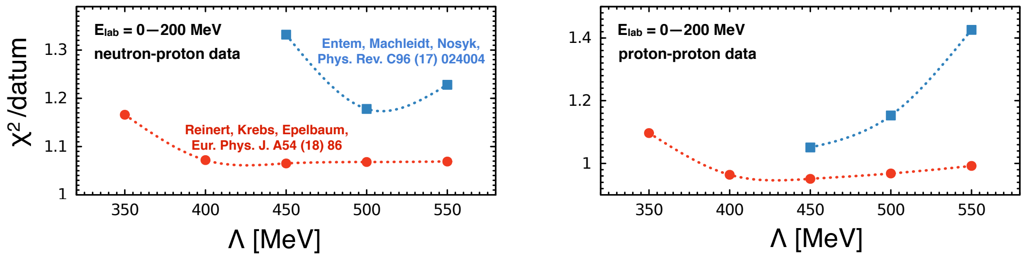

Figure 1: The dependence of χ^2 per datum for the description of the np and pp data in the energy range of $E_{\mathrm{lab}} = 0-200$ MeV from the 2013 Granada data base using the N^{4}LO$^+$ chiral potentials of Ref. [1] (red circles) and Ref. [15] (blue squares) for all available cutoff values.

estimation of statistical error, truncation error using the approach of Ref. [2], uncertainty in the πN LECs and uncertainty in the choice of the maximum energy in the fits, in order.

While the N^{4}LO$^+$ potentials of Ref. [1] provide a nearly perfect description of the available scattering data, the treatment of isospin breaking effects in that paper is still incomplete and essentially the same as in the older Nijmegen PWA of Ref. [38]. Work is in progress towards PWA of NN data including a more complete treatment of isospin-breaking interactions, which have been derived in Ref. [39] consistently with the isospin-invariant potentials employed in our analysis, see Ref. [40]. This study is expected to shed light on the long-standing discussion in connection with a possible charge dependence of the πN coupling constant, see Ref. [41] for a recent review.

3. Beyond the two-nucleon system

Motivated by the success of chiral EFT in the description of NN scattering data, it is of great interest to push chiral EFT to high orders for three- and more-nucleon systems. With most of the parameters entering the nuclear Hamiltonian being fixed in the NN system, this will allow for highly nontrivial tests of the theory. At the same time, it may improve our understanding of the three-nucleon force (3NF), which is an important frontier in nuclear physics. This is, in fact, one of the main goals of the recently formed Low Energy Nuclear Physics International Collaboration (LENPIC).

Up to and including N^{4}LO, the nuclear Hamiltonian includes the contributions of the 3NF and four-nucleon forces, most of which have already been worked out [42, 43, 44, 45, 46, 47, 48, 49, 50, 51, 52, 53]. The numerical implementation of the 3NF in Faddeev-Yakubovsky equations and in most of the ab-initio methods for nuclear structure calculations requires performing partial wave decomposition (PWD) which represents a non-trivial task. Using an efficient numerical approach developed within the LENPIC Collaboration [54], see also Ref. [55], it is nowadays possible to perform PWD of arbitrary local contributions to the 3NF. The treatment of non-local terms is significantly more demanding in terms of the required computational time. Another challenge which still needs to be tackled concerns a *consistent* regularization of the 3NF. Here, the complication emerges from the fact that contrary to purely contact two- and three-nucleon operators, the momentum dependence of the few-nucleon contact interactions involving pions is constrained by the chiral symmetry. Therefore, using inconsistently regularized NN and 3N forces results in violations

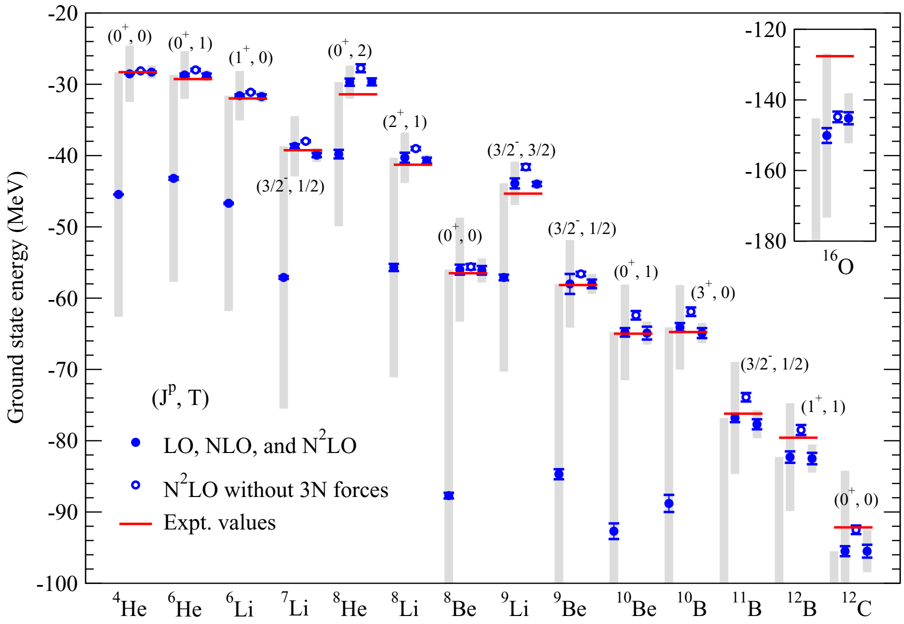

Figure 2: Calculated GS energies in MeV using chiral LO, NLO and N^{2}LO interactions with the coordinate-space cutoff of $R = 1.0$ fm in comparison with experimental values. For each nucleus, the LO, NLO, and N^{2}LO results are the left, middle, and right symbols and bars, respectively. The open blue symbols correspond to incomplete calculations at N^{2}LO using NN-only interactions. Blue error bars indicate the extrapolation uncertainty of the no-core configuration interaction method and, where applicable, an estimate of the similarity renormalization group (SRG) parameter dependence. The shaded bars indicate the estimated truncation error following Ref. [4].

of the chiral symmetry. This issue becomes nontrivial starting from N^{3}LO and is also relevant for calculations involving exchange currents [17].

Recently, we have analyzed nucleon-deuteron (Nd) scattering and selected properties of light nuclei up to next-to-next-to-leading order (N^{2}LO) using the novel semi-local NN potentials of Refs. [2, 3] along with the corresponding 3NF [7]. We used the ^{3}H binding energy to express one of the two LECs entering the 3NF at N^{2}LO (c_E) in terms of the second LEC c_D. To fix the letter one, we considered a broad range of Nd scattering observables including the neutron-deuteron doublet scattering length as well as the available experimental data on the differential and total cross sections at various energies. Taking into account the estimated truncation error at N^{2}LO, the strongest constraint on c_D is found to emerge from the experimental data of Ref. [56] for the differential cross section in the minimum area at the lowest considered energy of $E_{\rm lab} = 70$ MeV.

In Fig. 2 we show the resulting predictions for the ground state (GS) energies of nuclei with $A \leq 16$ at various chiral orders. It is reassuring to see that with only few exceptions, the inclusion of the 3NF leads to an improved description of the GS energies. For more results and comparison with the chiral EFT calculations see [7].

4. Bayesian truncation error estimation

The last topic I address in this contribution concerns the various approaches to estimate the truncation error, which in many cases dominates the uncertainty budget. Given the anticipated high accuracy level of chiral EFT, it is of utmost importance to develop a reliable approach for estimating the size of the neglected contributions from higher orders.

An important step along this line was made in Ref. [2] by establishing a simple and universally applicable algorithm to quantify the truncation error. Consider an observable $X(p)$, with p being the corresponding momentum scale, calculated up to the highest chiral order Q^i, $i = 0, 2, 3, 4, \ldots$. The expansion parameter Q was assumed to be

$$Q = \max\left(\frac{p}{\Lambda_b}, \frac{M_\pi}{\Lambda_b}\right), \tag{4.1}$$

and the breakdown scale was estimated from the error plots to be $\Lambda_b \sim 600$ MeV. The truncation error $\delta X^{(i)}$ at order Q^i was estimated in Ref. [2] via

$$\delta X^{(0)} = Q^2 |X^{(0)}|, \qquad \delta X^{(i)} = \max_{2\le j\le i}\left(Q^{i+1}|X^{(0)}|, Q^{i+1-j}|\Delta X^{(j)}|\right) \text{ with } i \ge 2, \tag{4.2}$$

with $\Delta X^{(2)} \equiv X^{(2)} - X^{(0)}$ and $\Delta X^{(i)} \equiv X^{(i)} - X^{(i-1)}$, subject to the additional constraint $\delta X^{(i)} \ge \max\limits_{j,k}\left(\left|X^{(j\ge i)} - X^{(k\ge i)}\right|\right)$. This simple approach does not rely on cutoff variation, which does not allow for a reliable estimation of the truncation error [2], and it can be applied to any observable of interest for any particular choice of the regulator. However, it does not directly allow for a statistical interpretation of the estimated uncertainties.

In Refs. [11, 12, 13], this algorithm was re-interpreted, further developed and statistically validated using the Bayesian approach. The main ingredients of these analyses are the coefficients c_n in the chiral expansion of X, $X = X_{\rm ref}\sum_{n=0}^{\infty} c_n Q^n$ (with $c_1 = 0$). For the calculated chiral orders $n \le i$, these coefficients are known and can be extracted from $\Delta X^{(n)}$. In Ref. [12], the LO coefficient c_0 was used to set the overall scale. The naturalness assumption was implemented by treating $c_i = (c_2, c_3, \ldots, c_i)$ as random variables with some probability distribution characterized by the upper bound $\bar{c}$. Performing marginalization over the h neglected orders subject to the assumed prior $\rm pr(c_n|\bar{c})$, the authors of Ref. [12] estimate the truncation error $\delta X^{(i)}$, assuming $\delta X^{(i)} \simeq \sum_{n=i+1}^{i+h} c_n Q^n \equiv \Delta$, by calculating the probability distribution $\rm pr_h(\Delta|c_i)$ for Δ given the known values of the coefficients c_i. It was shown in Ref. [11] that the approach in Eq. (4.2) introduced in Ref. [2] emerges from a particular class of naturalness priors, and the resulting uncertainties are consistent with the 68% degree-of-belief (DoB) intervals.

The Bayesian approach also allows to perform consistency checks of the assumed statistical model for the error by comparing the actual success rate of estimating the size of the higher-order contributions[2] with the expectations based on the DoB intervals. In Ref. [11], the consistency of the estimation for the breakdown scale $\Lambda_b = 600$ MeV was tested using the np total cross section at four different energies for the potentials of Ref. [2, 3]. For the optimal value of the coordinate-space cutoff $R = 0.9$ fm, it was found that while $\Lambda_b = 600$ MeV is statistically consistent, it may

[2]The estimation is regarded successful if the next-higher-order correction falls within the estimated uncertainty.

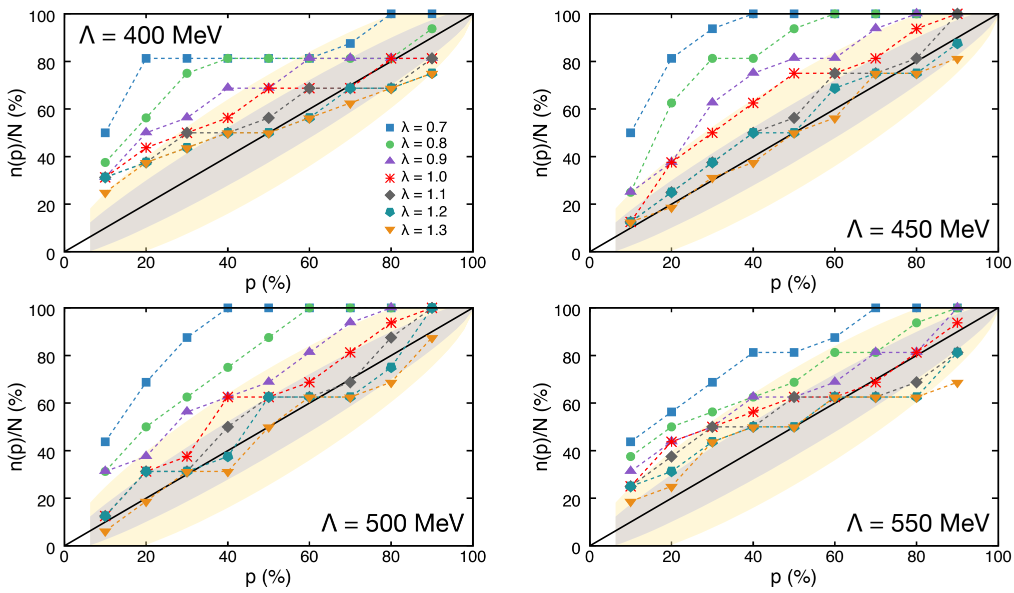

Figure 3: Empirical determination of the rescaling parameter λ of the breakdown scale Λ_b ($\lambda = 1$ corresponds to $\Lambda_b = 600$ MeV) for the potentials of Ref. [1] based on the total cross section at $E_{\rm lab} = 100$, 150, 200 and 250 MeV and the prior set $C^{(10)}_{0.25-10}$. The shaded bands represent 68% and 95% confidence intervals for the success rates.

be somewhat too conservative. This analysis was further developed and extended using a larger set of observables in Ref. [12] for the same chiral potentials.

In this contribution we apply the Bayesian approach of Ref. [12] to statistically "tune" the model for the expansion parameter Q in Eq. (4.1) using the most recent chiral NN potentials of Ref. [1] at the cutoff values of $\Lambda = \{400, 450, 500, 550\}$ MeV.[3] Following [12], we employ the Gaussian prior C, $\mathrm{pr}(\mathrm{c_n}|\bar{\mathrm{c}}) = \frac{1}{\sqrt{2\pi}\bar{\mathrm{c}}} \exp(-\mathrm{c_n^2}/2\bar{\mathrm{c}}^2)$ with $\mathrm{pr}(\bar{\mathrm{c}}) = \frac{1}{\ln \bar{\mathrm{c}}_>/\bar{\mathrm{c}}_<} \frac{1}{\bar{\mathrm{c}}} \theta(\bar{\mathrm{c}} - \bar{\mathrm{c}}_<)\theta(\bar{\mathrm{c}}_> - \bar{\mathrm{c}})$ and choose $h = 10$, $c_< = 0.25$ and $c_> = 10$. The analytical result for the posterior probability distribution $\mathrm{pr}_{\mathrm{h}}^{(\mathrm{C})}(\Delta|c_{\mathrm{i}})$ is given in Eq. (A9) of that paper.

In a close analogy to Refs. [11, 12], we calculate the success rate for the total cross section at $E_{\rm lab} = 100$, 150, 200 and 250 MeV using rescaled values of the breakdown scale $\Lambda_b \to \lambda \Lambda_b$, $\lambda = 0.7, 0.8, \ldots, 1.3$. The corresponding consistency plots based on 16 observables (we test the predictions at NLO, N^{2}LO, N^{3}LO and N^{4}LO and treat N^{4}LO$^+$ results as incomplete N^{5}LO predictions) are shown in Fig. 3 for all considered cutoff values. The obtained results suggest the breakdown scale of the order of $\Lambda_b \sim 650 \ldots 700$ MeV which agrees with the findings of Ref. [11] and is somewhat larger than the value of $\Lambda_b \sim 600$ MeV recommended in [2].

Having determined the breakdown scale Λ_b one may, in the second step, empirically test the identification of the soft scale in Eq. (4.1) with the pion mass. Notice that while the assumed model for the expansion parameter does qualitatively capture the pattern observed in the error plots in Fig. 5 of Ref. [2] and Fig. 5 of Ref. [57], the NDA-based estimation for the expansion parameter of M_π/Λ_b cannot account for dimensionless factors. Moreover, given that (i) the one-pion exchange potential appears in a closed form which does not rely on the chiral expansion and (ii) some partial

[3] We do not include the softest cutoff choice of $\Lambda = 350$ MeV as it already leads to significant artifacts.

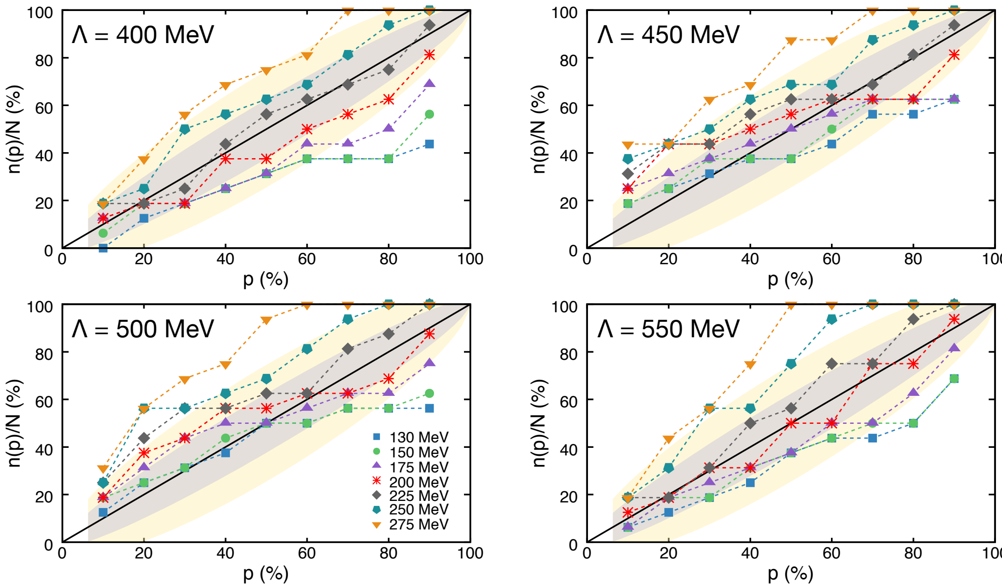

Figure 4: Empirical determination of the scale $M_\pi^{\rm eff}$ for the potentials of Ref. [1] based on the total cross section at $E_{\rm lab} = 5$, 25, 50 and 75 MeV and the prior set $C^{(10)}_{0.25-10}$. The shaded bands represent 68% and 95% confidence intervals for the success rates.

waves like e.g. the $^1S_0$ one are actually driven by two-pion exchange, the scale $M_\pi^{\rm eff}$ which controls the convergence rate of the expansion around the chiral limit for nuclear forces in Eq. (4.1) may actually be larger than M_π in line with the error plots shown in Refs. [2]. It, therefore, appears natural to determine the value of $M_\pi^{\rm eff}$ empirically. To this aim, we calculate the success rate for the total cross section at low energies of $E_{\rm lab} = 5$, 25, 50 and 75 MeV for different values of $M_\pi^{\rm eff}$ as visualized in Fig. 4. The consistency plots suggest the value of $M_\pi^{\rm eff} \sim 200$ MeV.

As an example, we show in Fig. 5 the N^{4}LO$^+$ results for np P-waves from Ref. [1] for $\Lambda = 450$ MeV along with the estimated N^{4}LO truncation errors using $M_\pi^{\rm eff} = 200$ MeV and $\Lambda_b = 700$ MeV. A comparison with Fig. 16 of Ref. [1] shows that the truncation errors estimated in that paper for these phase shifts correspond to $\sim 68\%$ or slightly larger DoB intervals.

5. Summary and outlook

In summary, considerable progress has been made towards developing chiral EFT into a precision tool for low-energy nuclear physics. While the two-nucleon sector of chiral EFT is already in a good shape, the chiral expansion of the three-nucleon force and nuclear currents still has to be pushed to N^{4}LO in order to match the accuracy of the high-precision NN chiral potentials. Special attention has to be paid to regularization of the many-body forces and exchange current operators, which should be carried out consistently with the NN potentials. The resulting nuclear forces and currents will allow to perform nontrivial tests of chiral EFT and are expected to shed light on the long-standing three-body force problem in nuclear physics.

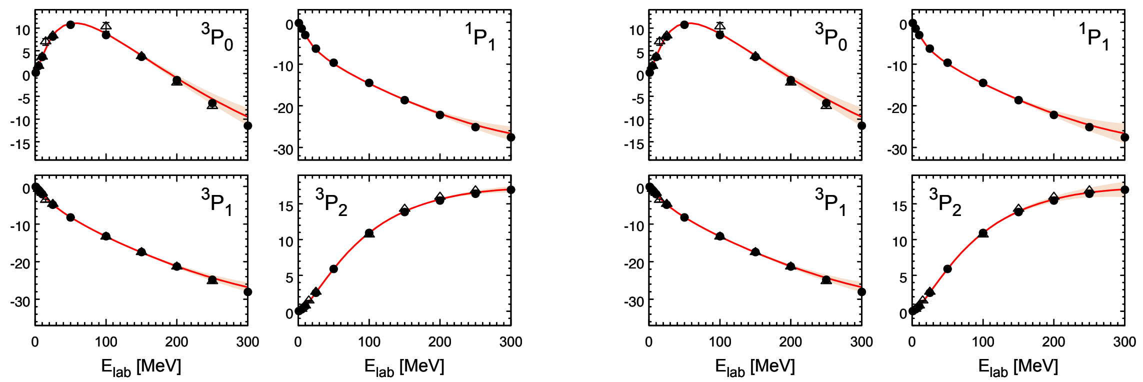

Figure 5: N^{4}LO$^+$ results for np P-waves of Ref. [1] with $\Lambda = 450$ MeV along with the estimated N^{4}LO truncation error bands (68% DoB) using the prior set $C^{(10)}_{0.25-10}$ (left panel) and the less informative prior set $C^{(10)}_{\epsilon}$ which marginalizes over $\bar{c}$ (right panel).

References

[1] P. Reinert, H. Krebs and E. Epelbaum, Eur. Phys. J. A **54**, no. 5, 86 (2018).

[2] E. Epelbaum, H. Krebs and U.-G. Meißner, Eur. Phys. J. A **51**, no. 5, 53 (2015).

[3] E. Epelbaum, H. Krebs and U.-G. Meißner, Phys. Rev. Lett. **115**, no. 12, 122301 (2015).

[4] S. Binder *et al.* [LENPIC Collaboration], Phys. Rev. C **93**, no. 4, 044002 (2016).

[5] R. Skibiński *et al.*, Phys. Rev. C **93**, no. 6, 064002 (2016).

[6] S. Binder *et al.* [LENPIC Collaboration], Phys. Rev. C **98**, no. 1, 014002 (2018).

[7] E. Epelbaum *et al.* [LENPIC Collaboration], Phys. Rev. C **99**, no. 2, 024313 (2019).

[8] D. Siemens *et al.*, Phys. Rev. C **94**, no. 1, 014620 (2016).

[9] D. L. Yao *et al.*, JHEP **1605**, 038 (2016).

[10] D. Siemens *et al.*, Phys. Rev. C **96**, no. 5, 055205 (2017).

[11] R. J. Furnstahl, N. Klco, D. R. Phillips and S. Wesolowski, Phys. Rev. C **92**, no. 2, 024005 (2015).

[12] J. A. Melendez, S. Wesolowski and R. J. Furnstahl, Phys. Rev. C **96**, no. 2, 024003 (2017).

[13] S. Wesolowski, R. J. Furnstahl, J. A. Melendez and D. R. Phillips, arXiv:1808.08211 [nucl-th].

[14] E. Epelbaum, W. Glöckle and U.-G. Meißner, Nucl. Phys. A **747**, 362 (2005).

[15] D. R. Entem, R. Machleidt and Y. Nosyk, Phys. Rev. C **96**, no. 2, 024004 (2017).

[16] D. R. Entem and R. Machleidt, Phys. Rev. C **68**, 041001 (2003).

[17] H. Krebs, these proceedings.

[18] A. Dyhdalo, R. J. Furnstahl, K. Hebeler and I. Tews, Phys. Rev. C **94**, no. 3, 034001 (2016).

[19] M. Hoferichter *et al.*, Phys. Rev. Lett. **115**, no. 19, 192301 (2015).

[20] R. Navarro Perez, J. E. Amaro and E. Ruiz Arriola, Phys. Rev. C **88**, no. 6, 064002 (2013) Erratum: [Phys. Rev. C **91**, no. 2, 029901 (2015)].

[21] R. Skibiński, Y. Volkotrub, J. Golak, K. Topolnicki and H. Witała, Phys. Rev. C **98**, 014001 (2018).

[22] R. Machleidt, Phys. Rev. C **63**, 024001 (2001).

[23] V. G. J. Stoks, R. A. M. Klomp, C. P. F. Terheggen and J. J. de Swart, Phys. Rev. C **49**, 2950 (1994).

[24] G. P. Lepage, nucl-th/9706029.

[25] E. Epelbaum and U.-G. Meißner, Few Body Syst. **54**, 2175 (2013).

[26] E. Epelbaum and J. Gegelia, Eur. Phys. J. A **41**, 341 (2009).

[27] E. Epelbaum and J. Gegelia, PoS CD **09**, 077 (2009).

[28] E. Marji *et al.*, Phys. Rev. C **88**, no. 5, 054002 (2013).

[29] E. Epelbaum *et al.*, Eur. Phys. J. A **54**, no. 11, 186 (2018).

[30] E. Epelbaum and J. Gegelia, Phys. Lett. B **716**, 338 (2012).

[31] E. Epelbaum and J. Gegelia, PoS CD **12**, 090 (2013).

[32] E. Epelbaum, A. M. Gasparyan, J. Gegelia and M. R. Schindler, Eur. Phys. J. A **50**, 51 (2014).

[33] V. Baru *et al.*, Phys. Rev. D **92**, no. 11, 114016 (2015).

[34] K. W. Li, X. L. Ren, L. S. Geng and B. Long, Phys. Rev. D **94**, no. 1, 014029 (2016).

[35] J. Song, K. W. Li and L. S. Geng, Phys. Rev. C **97**, no. 6, 065201 (2018).

[36] E. Epelbaum, A. M. Gasparyan, J. Gegelia and H. Krebs, Eur. Phys. J. A **51**, no. 6, 71 (2015).

[37] P. W. Lisowski *et al.*, Phys. Rev. Lett. **49**, 255 (1982).

[38] V. G. J. Stoks, R. A. M. Klomp, M. C. M. Rentmeester and J. J. de Swart, Phys. Rev. C **48**, 792 (1993).

[39] E. Epelbaum and U.-G. Meißner, Phys. Rev. C **72**, 044001 (2005).

[40] P. Reinert, these proceedings.

[41] E. Matsinos, arXiv:1901.01204 [nucl-th].

[42] S. Weinberg, Nucl. Phys. B **363**, 3 (1991).

[43] U. van Kolck, Phys. Rev. C **49**, 2932 (1994).

[44] E. Epelbaum *et al.*, Phys. Rev. C **66**, 064001 (2002).

[45] E. Epelbaum, Phys. Lett. B **639**, 456 (2006).

[46] E. Epelbaum, Eur. Phys. J. A **34**, 197 (2007).

[47] S. Ishikawa and M. R. Robilotta, Phys. Rev. C **76**, 014006 (2007).

[48] V. Bernard, E. Epelbaum, H. Krebs and U.-G. Meißner, Phys. Rev. C **77**, 064004 (2008).

[49] V. Bernard, E. Epelbaum, H. Krebs and U.-G. Meißner, Phys. Rev. C **84**, 054001 (2011).

[50] L. Girlanda, A. Kievsky and M. Viviani, Phys. Rev. C **84**, 014001 (2011).

[51] H. Krebs, A. Gasparyan and E. Epelbaum, Phys. Rev. C **85**, 054006 (2012).

[52] H. Krebs, A. Gasparyan and E. Epelbaum, Phys. Rev. C **87**, no. 5, 054007 (2013).

[53] E. Epelbaum, A. M. Gasparyan, H. Krebs and C. Schat, Eur. Phys. J. A **51**, no. 3, 26 (2015).

[54] J. Golak *et al.*, Eur. Phys. J. A **43**, 241 (2010).

[55] K. Hebeler, H. Krebs, E. Epelbaum, J. Golak and R. Skibiński, Phys. Rev. C **91**, no. 4, 044001 (2015).

[56] K. Sekiguchi *et al.*, Phys. Rev. C **65**, 034003 (2002).

[57] E. Epelbaum, PoS CD **15**, 014 (2016).